Ann Nucl Med
DOI 10.1007/s12149-016-1115-6

ORIGINAL ARTICLE

Automated quantification of amyloid positron emission tomography: a comparison of PMOD and MIMneuro

Woo Hee Choi[1] · Yoo Hyun Um[2] · Won Sang Jung[1] · Sung Hoon Kim[3]

Received: 8 June 2016 / Accepted: 1 August 2016

Abstract
Objective The aim of this study was to examine and compare two automated quantitative software tools (PMOD and MIMneuro) for the quantification of amyloid positron emission tomography (PET).
Methods A total of 30 subjects—15 Alzheimer's disease (AD) patients and 15 cognitively normal age- and sex-matched controls—were enrolled. All subjects underwent structural volumetric magnetic resonance imaging (MRI) and amyloid PET scans with F-18 florbetaben. Regional standardized uptake value ratios (SUVRs) using the cerebellar cortex as a reference region were obtained using PMOD and MIMneuro.
Results The SUVRs using both PMOD and MIMneuro showed high discriminatory power between the AD patients and cognitively normal controls. While PMOD and MIMneuro yielded significantly different SUVRs in some brain regions, the two methods had good overall agreement.
Conclusion MIMneuro provides comparable performance to PMOD without the need to acquire brain MRI. Therefore, MIMneuro might be suitable for clinical use to determine amyloid positivity.

✉ Sung Hoon Kim
nm@cmcnu.or.kr

[1] Department of Radiology, St. Vincent's Hospital, College of Medicine, The Catholic University of Korea, Suwon, Republic of Korea

[2] Department of Psychiatry, St. Vincent's Hospital, College of Medicine, The Catholic University of Korea, Suwon, Republic of Korea

[3] Department of Radiology, Seoul St. Mary's Hospital, College of Medicine, The Catholic University of Korea, 222 Banpo-daero, Seocho-gu, Seoul 137-701, Republic of Korea

Keywords Quantification · Florbetaben · PET · β-Amyloid · Alzheimer's disease

Introduction

Amyloid plaque deposition in the brain is a primary pathology of Alzheimer's disease (AD) [1]. Positron emission tomography (PET) tracers with high affinities for amyloid β (Aβ) plaques allow for the in vivo assessment of cortical amyloid burden [2], which was previously possible only at autopsy. Since F-18-labeled amyloid tracers were approved by the US Food and Drug Administration (FDA) for clinical use, amyloid PET imaging has been widely applied in clinical practice as well as AD studies [3–5].

Although visually rating amyloid PET is relatively simple and is the standard in clinical practice, quantification is often used to support standard visual reads in borderline cases and to monitor changes over time. Recently, pharmacologic research in AD has focused on the development of disease-modifying drugs that interfere with amyloid deposition. These clinical trials have used amyloid PET as a surrogate marker for study eligibility and for disease monitoring [6, 7]. Because the effects of anti-amyloid treatment on the PET signal are subtle, it is difficult to detect signal changes using only visual comparison [6, 7]. Therefore, accurate and reproducible quantification of brain amyloid burden is crucial for monitoring treatment efficacy.

Quantitative assessment of amyloid PET often relies on the computation of standardized uptake value ratios (SUVRs), which are ratios of activity in brain regions demonstrating high amyloid burden to that in a reference region with a low likelihood of amyloid deposition. Several software tools that automatically identify brain volumes of

Published online: 27 August 2016

interest (VOIs) and quantify regional amyloid load, such as Statistical Parametric Mapping (SPM), PMOD, and FreeSurfer, have been used in many studies. These software tools use the structural magnetic resonance imaging (MRI) data from each participant to calculate SUVRs, except for SPM, which can obtain SUVRs with or without MRI data. Acquiring additional MRI images increases time and cost. Furthermore, these tools are not easy to handle, and analysis processes take from tens of minutes to tens of hours. MIMneuro is a recently developed software package for clinical use that automatically quantifies regional amyloid load. MIMneuro computes regional SUVRs using PET imaging data without a need for structural T1-weighted MRI data. This is an important advantage when obtaining an appropriate brain MRI is not feasible. Amyloid PET quantification that does not require brain MRI simplifies image processing and reduces time and cost. However, MIMneuro has not undergone a rigorous peer-review process to establish its validity and suitability for diagnosis. To our knowledge, no study has compared MIMneuro to other established research methods. The aim of this study was thus to examine and compare MIMneuro to PMOD, an established research method, in terms of its ability to quantify amyloid PET.

Materials and methods

Subjects

This retrospective study included 15 AD patients (75.0 ± 9.2 years; 6 male, 9 female; Korean version of mini-mental state examination (MMSE) [8] score 17.6 ± 4.4; clinical dementia rating (CDR) [9] score 1.3 ± 0.5) and 15 cognitively normal age- and sex-matched controls (73.8 ± 6.5 years; 6 male, 9 female; MMSE score 26.9 ± 0.9; CDR score 0 ± 0) who were recruited from the outpatient psychiatric clinic of St. Vincent's Hospital of The Catholic University Korea. The AD patient group fulfilled the National Institute of Neurological and Communicative Disorders and Stroke and the Alzheimer's Disease and Related Disorders Association criteria for probable AD [10] and had a score on the CDR score of ≥1 [9]. We excluded subjects who had other neurologic or psychiatric conditions (including other forms of dementia or depression) and those taking any psychotropic medications (e.g., cholinesterase inhibitors, antidepressants, benzodiazepines, and antipsychotics). All participants underwent a neuropsychological assessment, brain MRI, and amyloid PET/computed tomography (CT) using F-18 florbetaben.

The study was conducted in accordance with the ethical and safety guidelines set forth by the institutional review board of our institution. The ethical committee of our institution does not require patient consent for retrospective review of imaging studies.

Image data acquisition

Amyloid PET

Combined PET/CT in-line systems (Gemini TF, Philips Healthcare, Best, The Netherlands) were used to acquire all data. An average of 300 MBq florbetaben was injected intravenously, and scanning began 90 min later. A low-dose CT scan was performed for attenuation correction and was immediately followed by PET imaging in three-dimensional (3D) mode for 20 min. The subject's head was immobilized with a head holder to minimize motion artifacts. Images were reconstructed using the standard ordered subset expectation maximization (OSEM) algorithm (subset 33, iteration 3).

MRI

All participants underwent MRI scans on a 3-T whole-body scanner equipped with an eight-channel phased-array head coil (Verio, Siemens, Erlangen, Germany). The scanning parameters of the T1-weighted 3D magnetization-prepared rapid gradient-echo (MPRAGE) sequences were as follows: echo time 2.5 ms, repetition time 1900 ms, inversion time 900 ms, flip angle 9.0°, field of view 250 × 250 mm, matrix 256 × 256, and voxel size 1.0 × 1.0 × 1.0 mm^3.

Image processing

PMOD-based analysis

All imaging data were processed using the PMOD PNEURO software tool (version 3.7, PMOD Technologies Ltd., Zürich, Switzerland). The 3D T1-weighted MRI images were automatically segmented into gray matter, white matter, and cerebrospinal fluid, and individual gray matter probability maps were calculated. The segmented MRI and PET images from each subject were co-registered, and then individual MRI images were normalized into the standard Montreal Neurological Institute (MNI) T1 template. The transformation parameters of the MR normalization were applied to the corresponding PET images. All images were visually checked for correct co-registration and appropriate segmentation. The automated anatomic labeling (AAL) atlas [11] was subsequently applied. The final VOI template for VOI analysis was obtained using the intersection of the atlas region with the gray matter probability map (mask threshold of 0.3). Some AAL VOIs were combined into the following seven VOIs for

quantitative analysis (Fig. 1): frontal cortex (F1O, F2O, F3O, FMO, and GR), lateral temporal cortex (T1, HES, T2, and T3), parietal cortex (P1, P2, and SMG), anterior cingulate (ACIN), posterior cingulate (PCIN), precuneus (PQ), and cerebellar cortex (cerebellum crus 1 and 2). Dividing the standardized uptake values of the regional VOIs by that of the cerebellar cortex as the reference region resulted in the regional SUVRs. The SUVRs for the six regions were then averaged together to generate the mean cortical SUVR.

MIM-based analysis

MIMneuro (version 6.3, MIM Software Inc., Cleveland, OH, USA) uses the "positive", "negative", and "average" florbetaben templates as the target for the florbetaben PET registration. These templates were created by aligning 10 positive and 10 negative scans to the Florbetapir PET templates. The first step is a nine-parameter affine registration, where the image is simultaneously aligned to three florbetaben PET templates ("positive", "negative", and "average"). This affine registration is then used to initialize a landmark-based thin-plate spline with deformable registration using several hundred landmarks located throughout the brain. This also optimizes the registration through image similarity metrics to all three templates simultaneously.

The MIM amyloid atlas was defined using 10 T1 MRI scans in conjunction with standard MIM contouring tools used by an anatomist and expert physicians in the field. The MRI scans were fused to the corresponding florbetaben PET scans for each patient. The florbetaben PET scans were then registered to template space using MIMneuro's multi-template deformable registration, and the same registration was applied to the MRI scan that was aligned to the florbetaben PET. This process allowed the MRI-defined atlas regions to be transformed to template space using the florbetaben PET deformable registration. The 10 contours for each structure were then combined using Majority Vote into a single atlas region where at least five of the 10 contours overlapped for that structure. In a similar manner, gray matter and white matter masks were defined on each T1 MRI using FreeSurfer, and the contours were transformed into template space using the deformable registration from an aligned florbetaben PET scan. Final gray matter and white matter contours were created from the overlap of at least five of the 10 corresponding contours in the template space. The white matter mask was then used to remove the white matter from each atlas contour to create the final gray matter atlas regions in the MIM amyloid atlas.

Analysis regions included the frontal cortex (inferior medial frontal gyrus), lateral temporal cortex, parietal cortex (superior parietal lobule), anterior cingulate, posterior cingulate, and precuneus (Fig. 1). As with PNEURO, regional SUVRs and mean cortical SUVR were calculated.

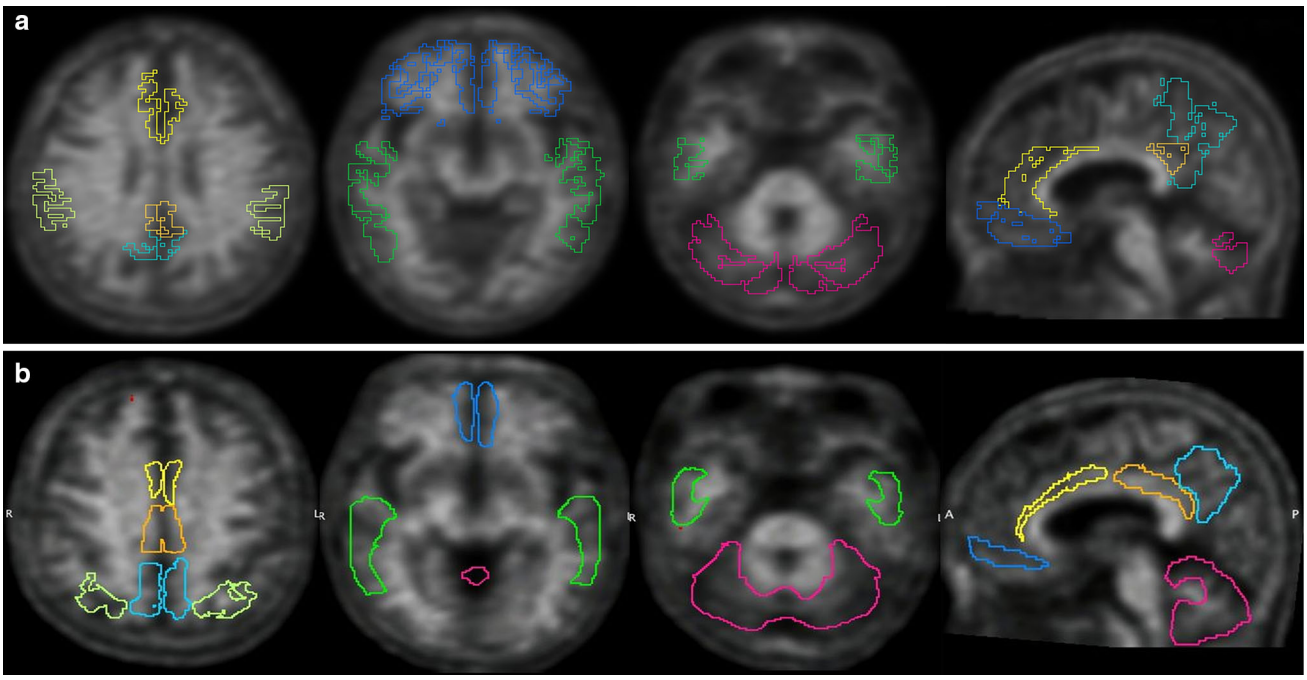

Fig. 1 Volumes of interest (VOIs) used in PMOD (**a**) and MIMneuro (**b**). VOIs were defined for the frontal cortex (*blue*), lateral temporal cortex (*green*), parietal cortex (*yellowish green*), anterior cingulate (*yellow*), posterior cingulate (*orange*), precuneus (*light blue*), and cerebellar cortex (*pink*)

Statistical analysis

Statistical analysis was performed using the statistical package for social sciences (SPSS) software (version 21.0, IBM Corp., Armonk, NY, USA) and MedCalc (version 12.2.1, MedCalc Software, Mariakerke, Belgium). Group differences in SUVRs were assessed using a Mann–Whitney *U* test. A Wilcoxon signed-rank test was used to compare the PMOD-based SUVRs with MIMneuro-based SUVRs. No correction for multiple comparisons was applied. Effect sizes of the SUVR differences between groups were expressed as Cohen's *d*. Receiver operating characteristic (ROC) analyses were used on mean cortical SUVRs to evaluate diagnostic power. Areas under the curve (AUCs) were calculated, and sensitivity and specificity were computed at the optimal cutoff points for both methods. The AUCs resulting from these ROC analyses were tested for differences according to the approach of DeLong and colleagues [12]. Correlations between SUVRs derived from PMOD and MIMneuro, and correlation between mean cortical SUVR and clinical parameters in AD patients were calculated using a Spearman correlation coefficient. Inter-rater reliability was assessed using an intraclass correlation coefficient (ICC) between PMOD and MIMneuro. A p value of <0.05 was considered statistically significant.

Results

For both methods, SUVRs in all brain VOIs were significantly higher in AD patients compared to cognitively normal controls (Table 1).

The effect sizes of SUVRs for group discrimination between the AD patients and cognitively normal controls using both methods are shown in Table 1. On a regional level, the best group discrimination was achieved by MIMneuro for lateral temporal cortex SUVR (Cohen's $d = 2.10$). The effect size of the mean cortical SUVR is higher for PMOD than for MIMneuro (Table 1).

In the AD patients, regional SUVR of the anterior cingulate was significantly lower using MIMneuro than PMOD, while SUVR of the precuneus was significantly higher using MIMneuro. In the cognitively normal controls, SUVRs of the anterior cingulate and the frontal cortex were significantly lower using MIMneuro than PMOD, whereas SUVRs of the parietal cortex were significantly higher using MIMneuro. There was no significant difference between mean cortical SUVRs obtained using either method for both AD patients and cognitively normal controls (Table 2). Regional SUVRs using both

Table 1 Comparison of SUVRs between patients with Alzheimer's disease and cognitively normal controls

	PMOD				MIMneuro			
	AD	NCs	*p*	*d*	AD	NCs	*p*	*d*
Frontal cortex	2.03 ± 0.33	1.45 ± 0.27	0.006	1.90	2.00 ± 0.35	1.31 ± 0.32	<0.001	2.03
Lateral temporal cortex	1.88 ± 0.30	1.35 ± 0.22	<0.001	2.05	1.84 ± 0.26	1.33 ± 0.23	<0.001	2.10
Parietal cortex	1.89 ± 0.31	1.36 ± 0.22	<0.001	1.99	1.94 ± 0.25	1.49 ± 0.23	<0.001	1.82
Anterior cingulate	1.92 ± 0.35	1.39 ± 0.28	<0.001	1.67	1.76 ± 0.41	1.30 ± 0.32	<0.001	1.24
Posterior cingulate	2.06 ± 0.36	1.45 ± 0.25	<0.001	1.99	2.09 ± 0.38	1.49 ± 0.27	<0.001	1.81
Precuneus	1.97 ± 0.36	1.37 ± 0.27	<0.001	1.91	2.05 ± 0.37	1.41 ± 0.31	<0.001	1.87
Mean cortical SUVR	1.96 ± 0.32	1.39 ± 0.24	<0.001	1.99	1.95 ± 0.32	1.39 ± 0.27	<0.001	1.88

AD patients with Alzheimer's disease, *NCs* cognitively normal controls, *p* statistical significance determined by Mann–Whitney *U* test, *d* Cohen's effect size

Table 2 Comparison between SUVRs calculated using two software tools

	AD ($n = 15$)			NCs ($n = 15$)		
	PMOD	MIMneuro	*p*	PMOD	MIMneuro	*p*
Frontal cortex	2.03 ± 0.33	2.00 ± 0.35	0.258	1.45 ± 0.27	1.31 ± 0.32	0.001*
Lateral temporal cortex	1.88 ± 0.30	1.84 ± 0.26	0.182	1.35 ± 0.22	1.33 ± 0.23	0.451
Parietal cortex	1.89 ± 0.31	1.94 ± 0.25	0.256	1.36 ± 0.22	1.49 ± 0.23	0.001*
Anterior cingulate	1.92 ± 0.35	1.76 ± 0.41	0.004*	1.39 ± 0.28	1.30 ± 0.32	0.008*
Posterior cingulate	2.06 ± 0.36	2.09 ± 0.38	0.328	1.45 ± 0.25	1.49 ± 0.27	0.125
Precuneus	1.97 ± 0.36	2.05 ± 0.37	0.006*	1.37 ± 0.27	1.41 ± 0.31	0.105
Mean cortical SUVR	1.96 ± 0.32	1.95 ± 0.32	0.551	1.39 ± 0.24	1.39 ± 0.27	0.889

AD patients with Alzheimer's disease, *NCs* cognitively normal controls, *p* statistical significance based on Wilcoxon signed-rank test, * $p < 0.05$

Table 3 Correlation between regional SUVRs as obtained by PMOD and MIMneuro

	AD (ρ)	NCs (ρ)
Frontal cortex	0.924	0.805
Lateral temporal cortex	0.936	0.878
Parietal cortex	0.928	0.838
Anterior cingulate	0.914	0.810
Posterior cingulate	0.870	0.914
Precuneus	0.953	0.922
Mean cortical SUVR	0.960	0.896

AD patients with Alzheimer's disease, *NCs* cognitively normal controls, ρ Spearman's rho, all correlations are significant at $p < 0.001$

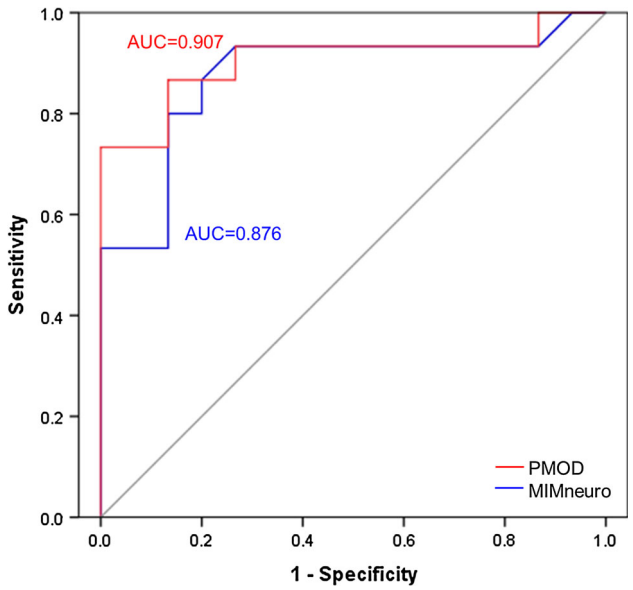

Fig. 2 Receiver operating characteristic (ROC) curves for mean cortical SUVRs obtained by PMOD and MIMneuro

methods were strongly correlated for all brain VOIs ($p < 0.001$) (Table 3).

To evaluate the ability of the mean cortical SUVRs from both methods to discriminate between AD patients and cognitively normal controls, the optimal cutoff values were determined using ROC analyses. The AUC was 0.907 for PMOD and 0.876 for MIMneuro (Fig. 2). The two compared areas were not significantly different ($p = 0.1969$). According to the ROC analyses, the optimal mean cortical SUVR cutoff value was 1.48 for PMOD and 1.50 for MIMneuro. Both methods had the same performance (sensitivity 93.3 %, specificity 73.3 %, negative predictive value 91.6 %, and positive predictive value 77.8 %). The ICC value for inter-rater reliability for both methods was calculated to be 0.99 ($p < 0.001$).

Correlation between mean cortical SUVR and clinical parameters (age, MMSE, and CDR) was also evaluated in AD patients (Table 4). The mean cortical SUVR derived using MIMneuro had a significant negative correlation with MMSE ($p = 0.35$), whereas the mean cortical SUVR derived using PMOD was not.

Table 4 Correlation between mean cortical SUVRs and clinical parameters in patients with Alzheimer's disease

	PMOD		MIMneuro	
	ρ	p	ρ	p
Age	0.475	0.074	0.457	0.087
MMSE	−0.435	0.105	−0.546	0.035*
CDR	0.349	0.202	0.349	0.202

MMSE mini-mental state examination, *CDR* clinical dementia rating, ρ Spearman's rho, * $p < 0.05$

Discussion

Lopresti et al. [13] proposed a simple method for the quantification of amyloid PET using SUVRs. This method has been widely used because it does not require dynamic scans or blood sampling. The regions for the SUVRs usually include cortical areas known to accumulate amyloid plaques (frontal, lateral temporal, parietal cortices, anterior, posterior cingulate, and precuneus) [14–16]. The cerebellar cortex is frequently used as a reference region because of its low levels or lack of neuritic plaques [17–19]. Early studies relied on manual delineation of VOIs for analysis [13, 20, 21]. However, this method is time consuming, especially for large datasets, and is less reproducible [22]. More recent studies have employed software, such as SPM [23–25], PMOD [26], and FreeSurfer [27, 28], to automatically identify brain VOIs and quantify regional amyloid load. Several studies have reported that SUVRs obtained using these software tools were in good agreement with those obtained by manually delineated VOIs [29–32]. PMOD PNEURO is a research-specific toolkit that has been widely used in amyloid PET research and covers all data processing steps, including spatial normalization, co-registration, brain segmentation, automated brain structure outlining, and brain VOI editing for image quantification [16, 19, 26, 33]. Tuszynsk et al. reported that quantification using PMOD allows for better discrimination between AD patients and healthy controls than other automated methods [29].

In this study, two software tools for automated quantification of amyloid PET were evaluated. PMOD employs the subject's own T1-weighted MR images for registration and delineation of VOIs while MIMneuro relies on standardized PET template registration. High uptake in the cerebral white matter has been reported in all amyloid PET tracers [2, 34–36] and is thought to be related to non-

specific binding to myelin [37]. Because the spillover from the adjacent white matter into gray matter can affect the quantification of SUVRs, gray matter masks were used. An individual gray matter mask derived from the segmentation of the subject's MRI scan was employed in PMOD, whereas a normalized mask was used in MIMneuro. Therefore, the template-based quantification used in MIMneuro may not fully avoid white matter interference. The impact of the spillover may be prominent in normal controls where there is very little amyloid deposition in the cortical regions but very high non-specific binding in the white matter. Saint-Aubert et al. reported a significant increase in frontal, parietal, and posterior cingulate uptake using PET template-based quantification methods in healthy controls compared to individual MRI-based methods [38]. Edison et al. also reported that mean SUVRs from a template-based method in healthy controls were significantly greater than those from an MRI-based method in all cortical regions [39]. Our study indicated that the SUVRs of the parietal cortex were significantly higher when a PET template-based method (MIMneuro) was used, while the SUVRs of the anterior cingulate and the frontal cortex were significantly lower than those obtained using an MRI-based method (PMOD) in cognitively normal controls. This discrepancy might be due to different definitions of VOIs. The VOIs for the anterior cingulate and frontal cortex used in MIMneuro are relatively small in size and are located in the medial portion, where the effects of white matter are relatively small (Fig. 1). Difference in SUVRs of the frontal cortex was not noted in the AD patients. This may be due to the highly specific binding of the amyloid tracer to the frontal gray matter, which would mask any spillover effect. However, the SUVRs of the precuneus were significantly higher when MIMneuro was used. This might be due to bias related to a small sample size or the specific binding of the amyloid tracer that would not be sufficient to conceal the spillover effect. Some differences may cancel each other out, resulting in no overall significant difference between the mean cortical SUVRs obtained using the two software tools in both groups.

There were strong correlations among the SUVRs obtained using both software tools for all brain regions. In accordance with a previous study [39], there was a better correlation in AD patients than in cognitively normal controls. This may be due to white matter uptake having less of an effect on SUVR calculations in AD patients compared to cognitively normal controls.

MMSE was significantly negatively correlated with mean cortical SUVR using MIMneuro, but not PMOD, in AD patients, though SUVRs obtained using both methods were strongly correlated ($\rho = 0.960$). This was possibly due to the small sample size.

The SUVRs obtained using both PMOD and MIMneuro had high discriminatory power when distinguishing between AD patients and cognitively normal controls. The SUVRs derived using both methods were significantly higher for the AD patients than for the cognitively normal controls, and effect sizes ranged from 1.24 to 2.10. The highest effect size for group discrimination was observed with the lateral temporal cortex SUVR obtained using MIMneuro. The AUC for MIMneuro was slightly smaller than the AUC for PMOD. However, MIMneuro had a 100 % classification accordance and equal diagnostic accuracy to PMOD. Furthermore, the inter-rater reliability between mean cortical SUVRs calculated using both methods was very high (ICC = 0.99). In conclusion, both PMOD and MIMneuro have very good overall agreement, even though differences in SUVRs may be observed for some regions.

Several previous studies comparing PET-only methods with MRI-based methods to quantify amyloid PET have demonstrated reliable performance of PET-only methods [39, 40]. However, Saint-Aubert et al. have suggested that an MRI-based approach shows greater difference between the AD group and the healthy control group [38]. In this study, both PMOD and MIMneuro provided comparable diagnostic performance despite some differences in absolute SUVRs. Because MIMneuro demonstrates good group discrimination between AD patients and cognitively normal controls, it may be considered a suitable tool for clinical diagnostic purposes. MRI segmentation takes time, and SUVRs cannot be calculated if MRI segmentation is inadequate, which can occur as frequently as in 5.5 % using PMOD [26]. Avoiding the need for MRI thus not only decreases cost, but also allows for more efficient analysis. MIMneuro is thus a good option for routine clinical studies, especially when individual MRI data are not available. However, subtle differences in SUVRs may be important in monitoring drug efficacy or during longitudinal follow-ups, where changes would be subtle. It remains to be investigated whether the two methods have comparable performance in detecting longitudinal changes and in monitoring the efficacy of anti-amyloid treatment. In addition, the sample size of this study was small. Thus, further studies using larger sample sizes are necessary.

In conclusion, MIMneuro provides comparable performance to PMOD, without the need for an additional MRI scan. Therefore, MIMneuro seems to be adequate for clinical use to determine amyloid positivity or to screen large study populations.

Compliance with ethical standards

Conflict of interest The authors have no conflicts of interest to declare.

References

1. Hardy J, Allsop D. Amyloid deposition as the central event in the aetiology of Alzheimer's disease. Trends Pharmacol Sci. 1991;12:383–8.
2. Klunk WE, Engler H, Nordberg A, Wang Y, Blomqvist G, Holt DP, et al. Imaging brain amyloid in Alzheimer's disease with Pittsburgh Compound-B. Ann Neurol. 2004;55:306–19.
3. FDA approves 18F-florbetapir PET agent. J Nucl Med. 2012;53:15n.
4. GE beta-amyloid agent approved. J Nucl Med. 2013;54:10n.
5. US Food and Drug Administration. Neuraceq (florbetaben F 18 injection): clinical pharmacology and biopharmaceutics review(s). 2014. http://www.fda.gov. Accessed 10 April 2016.
6. Rinne J, Brooks D, Rossor M, Fox N, Bullock R, Klunk W, et al. 11C-PiB PET assessment of change in fibrillar amyloid-beta load in patients with Alzheimer's disease treated with bapineuzumab: a phase 2, double-blind, placebo-controlled, ascending-dose study. Lancet Neurol. 2010;9:363–72.
7. Liu E, Schmidt M, Margolin R, Sperling R, Koeppe R, Mason N, et al. Amyloid-β 11C-PiB-PET imaging results from 2 randomized bapineuzumab phase 3 AD trials. Neurology. 2015;85:692–700.
8. Kang Y, Na DL, Hahn S. A validity study on the Korean Mini-Mental State Examination (K-MMSE) in dementia patients. J Korean Neurol Assoc. 1997;15:300–8.
9. Morris JC. The Clinical Dementia Rating (CDR): current version and scoring rules. Neurology. 1993;43:2412–4.
10. McKhann G, Drachman D, Folstein M, Katzman R, Price D, Stadlan EM. Clinical diagnosis of Alzheimer's disease: report of the NINCDS-ADRDA Work Group under the auspices of Department of Health and Human Services Task Force on Alzheimer's Disease. Neurology. 1984;34:939–44.
11. Tzourio-Mazoyer N, Landeau B, Papathanassiou D, Crivello F, Etard O, Delcroix N, et al. Automated anatomical labeling of activations in SPM using a macroscopic anatomical parcellation of the MNI MRI single-subject brain. Neuroimage. 2002;15:273–89.
12. DeLong ER, DeLong DM, Clarke-Pearson DL. Comparing the areas under two or more correlated receiver operating characteristic curves: a nonparametric approach. Biometrics. 1988;44:837–45.
13. Lopresti BJ, Klunk WE, Mathis CA, Hoge JA, Ziolko SK, Lu X, et al. Simplified quantification of Pittsburgh Compound B amyloid imaging PET studies: a comparative analysis. J Nucl Med. 2005;46:1959–72.
14. Braak H, Braak E. Neuropathological stageing of Alzheimer-related changes. Acta Neuropathol. 1991;82:239–59.
15. Thal DR, Rub U, Orantes M, Braak H. Phases of A beta-deposition in the human brain and its relevance for the development of AD. Neurology. 2002;58:1791–800.
16. Becker GA, Ichise M, Barthel H, Luthardt J, Patt M, Seese A, et al. PET quantification of 18F-florbetaben binding to beta-amyloid deposits in human brains. J Nucl Med. 2013;54:723–31.
17. Barthel H, Luthardt J, Becker G, Patt M, Hammerstein E, Hartwig K, et al. Individualized quantification of brain beta-amyloid burden: results of a proof of mechanism phase 0 florbetaben PET trial in patients with Alzheimer's disease and healthy controls. Eur J Nucl Med Mol Imaging. 2011;38:1702–14.
18. Svedberg MM, Hall H, Hellstrom-Lindahl E, Estrada S, Guan Z, Nordberg A, et al. [(11)C]PIB-amyloid binding and levels of Abeta40 and Abeta42 in postmortem brain tissue from Alzheimer patients. Neurochem Int. 2009;54:347–57.
19. Barthel H, Gertz HJ, Dresel S, Peters O, Bartenstein P, Buerger K, et al. Cerebral amyloid-beta PET with florbetaben (18F) in patients with Alzheimer's disease and healthy controls: a multicentre phase 2 diagnostic study. Lancet Neurol. 2011;10:424–35.
20. Pike K, Savage G, Villemagne V, Ng S, Moss S, Maruff P, et al. Beta-amyloid imaging and memory in non-demented individuals: evidence for preclinical Alzheimer's disease. Brain. 2007;130:2837–44.
21. Rowe CC, Ng S, Ackermann U, Gong SJ, Pike K, Savage G, et al. Imaging beta-amyloid burden in aging and dementia. Neurology. 2007;68:1718–25.
22. Destrieux C, Fischl B, Dale A, Halgren E. Automatic parcellation of human cortical gyri and sulci using standard anatomical nomenclature. Neuroimage. 2010;53:1–15.
23. Fleisher AS, Chen K, Liu X, Roontiva A, Thiyyagura P, Ayutyanont N, et al. Using positron emission tomography and florbetapir F18 to image cortical amyloid in patients with mild cognitive impairment or dementia due to Alzheimer disease. Arch Neurol. 2011;68:1404–11.
24. Joshi AD, Pontecorvo MJ, Clark CM, Carpenter AP, Jennings DL, Sadowsky CH, et al. Performance characteristics of amyloid PET with florbetapir F 18 in patients with alzheimer's disease and cognitively normal subjects. J Nucl Med. 2012;53:378–84.
25. Namiki C, Takita Y, Iwata A, Momose T, Senda M, Okubo Y, et al. Imaging characteristics and safety of florbetapir ((1)(8)F) in Japanese healthy volunteers, patients with mild cognitive impairment and patients with Alzheimer's disease. Ann Nucl Med. 2015;29:570–81.
26. Brendel M, Hogenauer M, Delker A, Sauerbeck J, Bartenstein P, Seibyl J, et al. Improved longitudinal [(18)F]-AV45 amyloid PET by white matter reference and VOI-based partial volume effect correction. Neuroimage. 2015;108:450–9.
27. Landau SM, Mintun MA, Joshi AD, Koeppe RA, Petersen RC, Aisen PS, et al. Amyloid deposition, hypometabolism, and longitudinal cognitive decline. Ann Neurol. 2012;72:578–86.
28. Landau SM, Fero A, Baker SL, Koeppe R, Mintun M, Chen K, et al. Measurement of longitudinal beta-amyloid change with 18F-florbetapir PET and standardized uptake value ratios. J Nucl Med. 2015;56:567–74.
29. Tuszynski T, Rullmann M, Luthardt J, Butzke D, Tiepolt S, Gertz HJ, et al. Evaluation of software tools for automated identification of neuroanatomical structures in quantitative beta-amyloid PET imaging to diagnose Alzheimer's disease. Eur J Nucl Med Mol Imaging. 2016;43:1077–87.
30. Rosario BL, Weissfeld LA, Laymon CM, Mathis CA, Klunk WE, Berginc MD, et al. Inter-rater reliability of manual and automated region-of-interest delineation for PiB PET. Neuroimage. 2011;55:933–41.
31. Su Y, D'Angelo GM, Vlassenko AG, Zhou G, Snyder AZ, Marcus DS, et al. Quantitative analysis of PiB-PET with FreeSurfer ROIs. PLoS One. 2013;8:e73377.
32. Schain M, Varnas K, Cselenyi Z, Halldin C, Farde L, Varrone A. Evaluation of two automated methods for PET region of interest analysis. Neuroinformatics. 2014;12:551–62.
33. Rullmann M, Dukart J, Hoffmann KT, Luthardt J, Tiepolt S, Patt M, et al. Partial-volume effect correction improves quantitative analysis of 18F-florbetaben beta-amyloid PET scans. J Nucl Med. 2016;57:198–203.
34. Villemagne VL, Ong K, Mulligan RS, Holl G, Pejoska S, Jones G, et al. Amyloid imaging with (18)F-florbetaben in Alzheimer disease and other dementias. J Nucl Med. 2011;52:1210–7.
35. Wong DF, Rosenberg PB, Zhou Y, Kumar A, Raymont V, Ravert HT, et al. In vivo imaging of amyloid deposition in Alzheimer disease using the radioligand 18F-AV-45 (florbetapir [corrected] F 18). J Nucl Med. 2010;51:913–20.
36. Vandenberghe R, Van Laere K, Ivanoiu A, Salmon E, Bastin C, Triau E, et al. 18F-flutemetamol amyloid imaging in Alzheimer

disease and mild cognitive impairment: a phase 2 trial. Ann Neurol. 2010;68:319–29.
37. Stankoff B, Freeman L, Aigrot MS, Chardain A, Dolle F, Williams A, et al. Imaging central nervous system myelin by positron emission tomography in multiple sclerosis using [methyl-(1)(1)C]-2-(4′-methylaminophenyl)-6-hydroxybenzothiazole. Ann Neurol. 2011;69:673–80.
38. Saint-Aubert L, Nemmi F, Peran P, Barbeau EJ, Payoux P, Chollet F, et al. Comparison between PET template-based method and MRI-based method for cortical quantification of florbetapir (AV-45) uptake in vivo. Eur J Nucl Med Mol Imaging. 2014;41:836–43.
39. Edison P, Carter SF, Rinne JO, Gelosa G, Herholz K, Nordberg A, et al. Comparison of MRI based and PET template based approaches in the quantitative analysis of amyloid imaging with PIB-PET. Neuroimage. 2013;70:423–33.
40. Landau SM, Breault C, Joshi AD, Pontecorvo M, Mathis CA, Jagust WJ, et al. Amyloid-beta imaging with Pittsburgh compound B and florbetapir: comparing radiotracers and quantification methods. J Nucl Med. 2013;54:70–7.